PROCEEDINGS OF SCIENCE

Design and construction status of the Mu2e crystal calorimeter

C. Bloise,[a] S. Ceravolo,[a] F. Cervelli,[b] F. Colao ,[a] M. Cordelli,[a] G. Corradi,[a] S. Di Falco,[b] E. Diociaiuti,[a] S. Donati,[b] C. Ferrari,[b] R. Gargiulo,[a] A. Gioiosa,[d] S. Giovannella,[a] V. Giusti,[b] D. Hampai,[a] F. Happacher,[a] M. Martini,[a] S. Miscetti,[a] L. Morescalchi,[b] D. Paesani,[a,*] D. Pasciuto,[b] E. Pedreschi,[b] F. Raffaelli,[b] E. Sanzani,[a] I. Sarra,[a] A. Saputi,[c] F. Spinella[b] and A. Taffara[b]

[a] *Laboratori Nazionali di Frascati dell'INFN, Frascati, Italy*
[b] *INFN - Sezione di Pisa, Italy*
[c] *INFN - Sezione di Ferrara, Italy*
[d] *Università degli Studi di Tor Vergata, Italy*

E-mail: daniele.paesani@lnf.infn.it

The Mu2e experiment at Fermilab will search for charged-lepton flavour violating neutrino-less conversion of negative muons into electrons in the coulomb field of Al nuclei. The conversion electron has a monoenergetic 104.967 MeV signature slightly below the muon mass and will be identified by a high-resolution tracker and an electromagnetic calorimeter (EMC), reaching a single event sensitivity of about 3×10^{-17}, four orders of magnitude beyond the current best limit. The calorimeter is composed of 1348 pure CsI crystals, each read by two custom UV-extended SiPMs, arranged in two annular disks. The EMC has high granularity, 10 % energy resolution and 500 ps timing resolution for 100 MeV electrons and will need to maintain extremely high levels of reliability and stability in a harsh operating environment with high vacuum, 1 T B-field and radiation exposures up to 100 krad and 10^{12} n_{1MeV}/cm^2. The calorimeter design, along with the custom front-end electronics, cooling and mechanical systems were validated through an electron beam test on a large-scale 51-crystals prototype (Module-0). Extensive test campaigns were carried out to characterise and verify the performance of crystals, photo-detectors, analogue and digital electronics, including hardware stress tests and irradiation campaigns with neutrons, protons, and photons. The production and quality control phases of all calorimeter components is about to be completed and the assembly of the downstream calorimeter disk is at an advanced state. A full vertical slice test with the final electronics was carried out on the Module-0, along with the implementation and validation of the calibration procedures.

41st International Conference on High Energy physics - ICHEP2022
6-13 July, 2022
Bologna, Italy

*Speaker

PoS(ICHEP2022)314

1. The Mu2e experiment at Fermilab

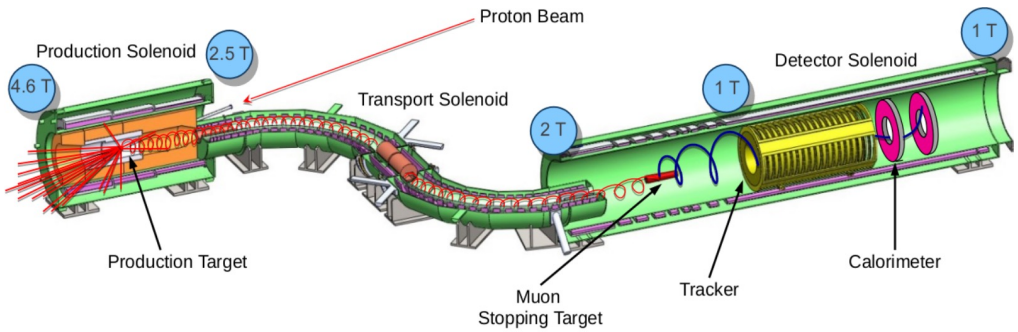

Figure 1: Schematic representation of the Mu2e experimental apparatus.

The Mu2e experiment [1] at Fermilab aims to improve by four orders of magnitude the current single event sensitivity for the yet unobserved charged-lepton flavour violating (CLFV) neutrinoless conversion of a negative muon into an electron in the field of an Al nucleus. Such process has a clear signature consisting in a mono-energetic 104.97 MeV conversion electron (CE), slightly below the muon mass. Assuming neutrino oscillations, CLFV processes in the muon system remain completely negligible, with BR($\mu \rightarrow e\,\gamma$) = 10^{-52} [2]. Observing CLFV candidates would then be a clear evidence of Physics beyond the Standard Model.

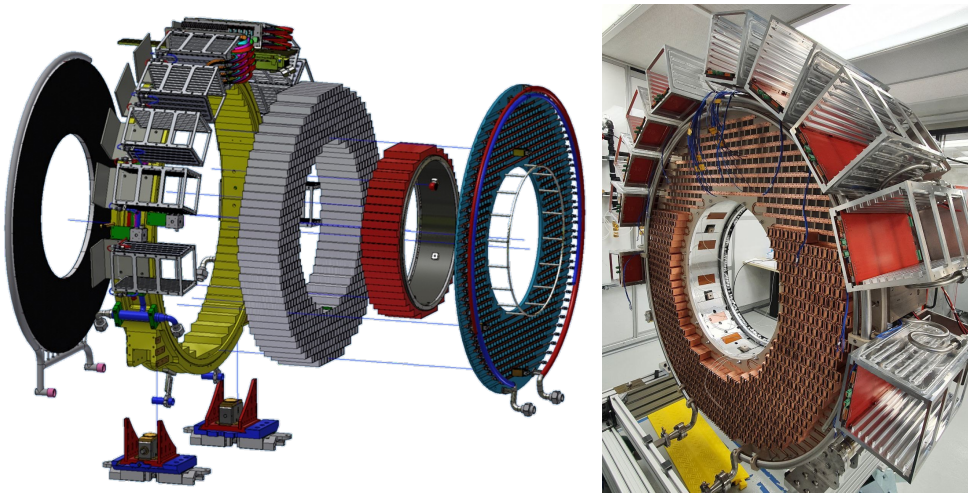

Figure 2: Left: exploded view of the Mu2e calorimeter. Right: downstream calorimeter disk under assembly at SiDet, Fermilab

The Mu2e experimental layout (Fig. 1) comprises a ~ 25 m long superconducting magnet system. In the Production Solenoid (PS), an 8 GeV pulsed proton beam impinges on a W target producing mostly pions, which are collected and focused by means of magnetic lenses into the Transport Solenoid (TS) to select and transport low-momentum negative muons from pion decays to the Detector Solenoid (DS). In the DS, muons will impinge at ~ 10 GHz on an Al stopping target and form muonic atoms, cascading to the 1S state. The bound muons can decay in-orbit (DIO) with

~ 39% relative probability or undergo nuclear capture with ~ 61% probability. Decay products are analysed by means of a high resolution straw-tube tracker [3] and an electromagnetic calorimeter [4]. To suppress fake CE events from cosmic muons, the DS and part of the TS are enclosed in a Cosmic Ray Veto (CRV) system. DIOs, along with fake candidates from cosmic rays, represent the main intrinsic background sources.

2. The Mu2e Crystal Calorimeter

Requirements and design. The Mu2e calorimeter [4] complements the tracker, providing cluster-based seeding for track finding at high occupancy, along with a stand-alone online trigger. Its particle identification capabilities provide a high μ/e rejection factor > 200. The calorimeter needs to guarantee (a) a large acceptance for CEs, (b) a position resolution (σ_{xy} < 1 cm), (c) an energy resolution < 10% and (d) a timing resolution < 500 ps for 100 MeV electrons [5]. The calorimeter will need to maintain extremely high levels of stability and reliability in harsh operating conditions featuring 10^{-4} mbar vacuum, 1 T magnetic field and a strong radiation environment, comprising ~ 90 krad Total Ionising Dose (TID) and 1.2×10^{12} n_{1MeV}/cm^2 total non-ionising dose (TNID) [6].

The calorimeter (Fig. 2) is composed of two disks, in order to maximise acceptance for CE tracks. Each disk houses a matrix of 674 parallelepipedal ($34 \times 34 \times 200$ mm^3) un-doped CsI crystals [7, 8]. Crystals must provide a light yield > 20 photo-electrons (p.e.)/MeV per SiPM and a scintillating decay time of ~ 40 ns to better cope with piled-up signals. Readout is performed via custom SiPM arrays, with UV-extended spectral responsivity (PDE > 20% down to 280 nm) to match the ~ 310 nm emission peak of pure CsI. A 2 mm gap is present between crystals and SiPMs to reduce their thermal coupling, preventing gradients along the crystal axis which could worsen their longitudinal response uniformity.

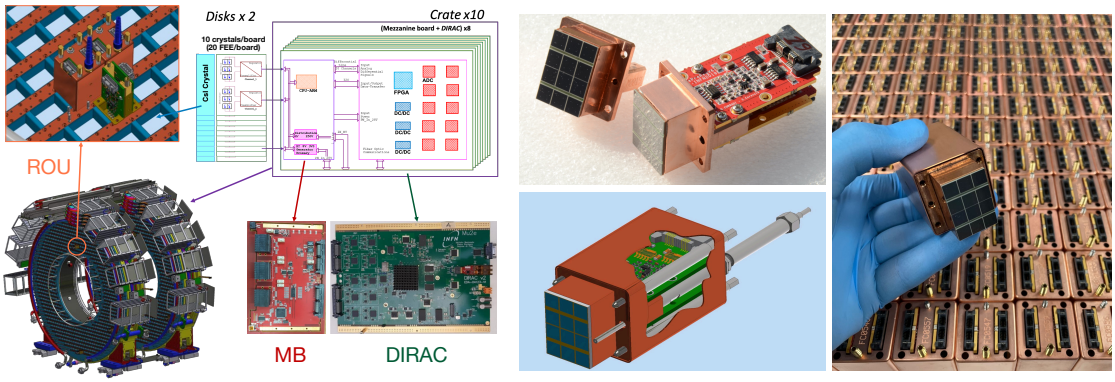

Figure 3: Overview of the Mu2e calorimeter readout system. Left: electronics crates architecture, including Mezzanine (MB) and DiRAC boards are also shown. Top-left: detail of the Read-Out Units (ROU) assembly in the calorimeter disk (heat exchangers are also visible). Right: rendering of a ROU, SiPM holder and FEE assembly, and photo of ROUs from production lots.

Readout chain. For redundancy and reliability reasons, a fully custom signal chain [6] provides a dual, fully independent readout system for each crystal, for a total of 1348 Read-out Units (ROU) installed behind the crystal matrices. Each ROU houses two custom large area UV-extended SiPM

arrays and the relative Front-end Electronics (FEE) boards, which perform signal amplification and shaping, along with onboard bias regulation and photosensor slow-control functions (bias voltage, current and temperature monitoring). SiPMs are glued on copper holders (Fig. 3), thermally coupled to the cooling system (Fig. 3, top-left) for their thermalisation down to -10°C, to cope with the TNID induced dark current increase. Dedicated electronics crates embedded in the calorimeter mechanical structure house a total of 136 microprocessor-controlled Mezzanine Boards (MB) - for power distribution and slow control management - and 136 DIgitiser ReAdout Controllers (DIRAC) - based on PolarFire FPGAs 12-bit Flash ADCs - which digitise all 2696 calorimeter channels at 200 Msps. A VTRX-based 10 Gsps optical link allows data stream and slow control management through the Mu2e Trigger and Data Acquisition System (TDAQ). Full signal digitisation allows to better cope with the high expected pile-up rates.

Calibration systems. A Fluorinert-based liquid radioactive source, externally activated by means of a DT neutron generator, is circulated through aluminium pipes installed on each disk cover plate to illuminate crystals with 6.13 MeV photons - obtained from a shortly lived ^{16}O transition - to calibrate their energy response. A second monitoring system is based on a 520 nm laser source, which is distributed via fibre-optic manifolds to each crystal for continuous photosensor gain monitoring and timing alignment. Additional calibration methods are based on crossing cosmic rays, electrons from μ^- DIO and positrons from stopped π^+ decays.

2.1 Calorimeter qualification and production status

Components production and qualification. Production and quality control were concluded in 2019 for a total of 4000 SiPMs with less than 2% out-of-spec components. In late 2019 and 2021 the production of, respectively, 1500 crystals and 3300 FEE boards were also successfully concluded. MB and DIRAC boards went also through their pre-production and prototyping phases and were truly tested in Vertical Slice Tests. Extensive qualification steps and quality controls were carried out on all components batches, including radiation hardness campaigns with ionising dose, and neutron sources, mainly at ENEA Calliope ^{60}Co photon source, and HZDR EPOS and ENEA-FNG neutron sources. Dedicated single-event effect (SEE) qualification campaigns are being carried out using proton beams on all electronic subsystems, as described elsewhere [6].

Read-out units. The assembly and test of the ROUs is in progress, and an automated testing station was developed at LNF-INFN. A 420 nm nanosecond UV LED source is pulsed at kHz repetition rate over two assembled production ROUs at a time. A motorised neutral density filter selector is used to vary the source intensity. SiPM response is calibrated - and stored in a dedicated ROU database - for different over-voltages and operating temperatures. An overall gain spread < 3% RMS was observed for production, with a 1.5% reproducibility in testing. A much detailed explanation of the station functionality and of its results can be found elsewhere [9].

First disk assembly. The final assembly of the downstream calorimeter disk begun in June 2022 in an ISO-7 class clean room located at SIDET, Fermilab (Fig. 2, right). After mechanics assembly and alignment, crystal stacking was started and completed in late July 2022. Crystal placement criteria was based on the selection of units with higher (lower) light yield, faster (slower) response and reduced (large) radiation-induced optical noise for the innermost (outermost) regions of each

disk, where more (less) intense radiation dose is expected. An additional constraint on crystal stacking and orientation was forced to compensate mechanical tolerances on crystal heights. ROU assembly and test with cosmic rays is being carried out at the moment of writing.

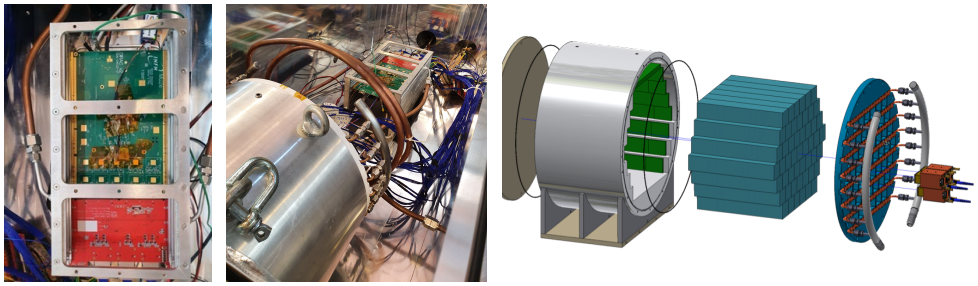

Figure 4: Center: VST setup with Module-0 and electronics crate. Left: detail of MB and DiRAC installed in the electronics crate. Right: Module-0 architecture.

3. Large scale prototype vertical slice test

In late 2021 a Vertical Slice Test (VST) of the full calorimeter readout chain was performed with cosmic muons at LNF-INFN on the calorimeter Module-0 [6] (Fig. 4, right), a large-scale prototype counting 51 crystals and designed with the final configuration of all detector services and subsystems (mechanics, cooling system, laser calibration system, vessel for vacuum operation). A dedicated Cosmic Ray Tagger (CRT) [10] constituted by two modules, each employing 8 fast scintillator bars with dual-sided SiPM readout, was also developed at LNF to track minimum-ionising particles inside the active volume of a calorimeter disk (or of the Module-0) for calibration purposes and verification of the longitudinal response of crystals. For the VST, an electronics crate with a DiRAC and a MB board were installed inside the Module-0 vacuum vessel to readout a total of 20 FEE channels (Fig. 4, center). The 17 innermost crystals were instrumented with production ROUs, and dual readout was used for the central, and the central uppermost/lowermost crystals.

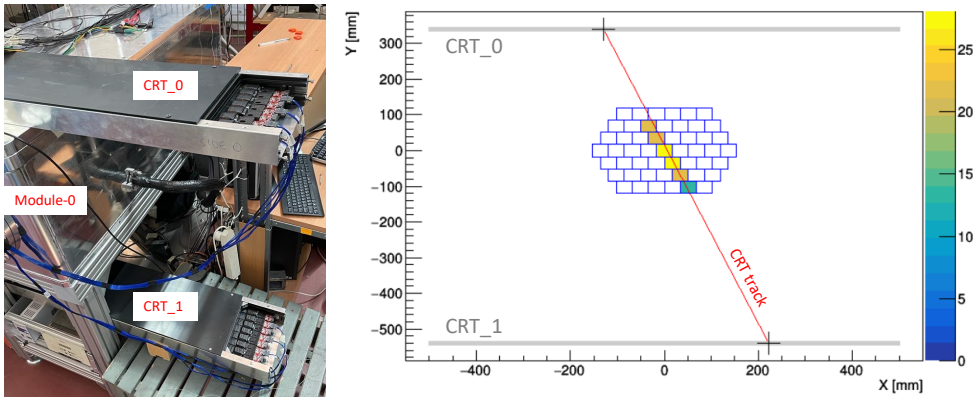

Figure 5: Left: VST setp using the two CRT modules. Right: minimum ionising cosmic track inside Module-0 with superimposed CRT trajectory.

Energy response was equalised online acting on SiPM biases to a level < 5 % and further offline equalisation was performed on the Minimum Ionizing Particles (MIP) most probable 21

MeV deposit (Fig. 6, top-left). SiPM gain stability was checked against the MIP peak, with its fluctuations being compatible with the ± 1°C stability of the temperature regulation system (Fig. 6, right).

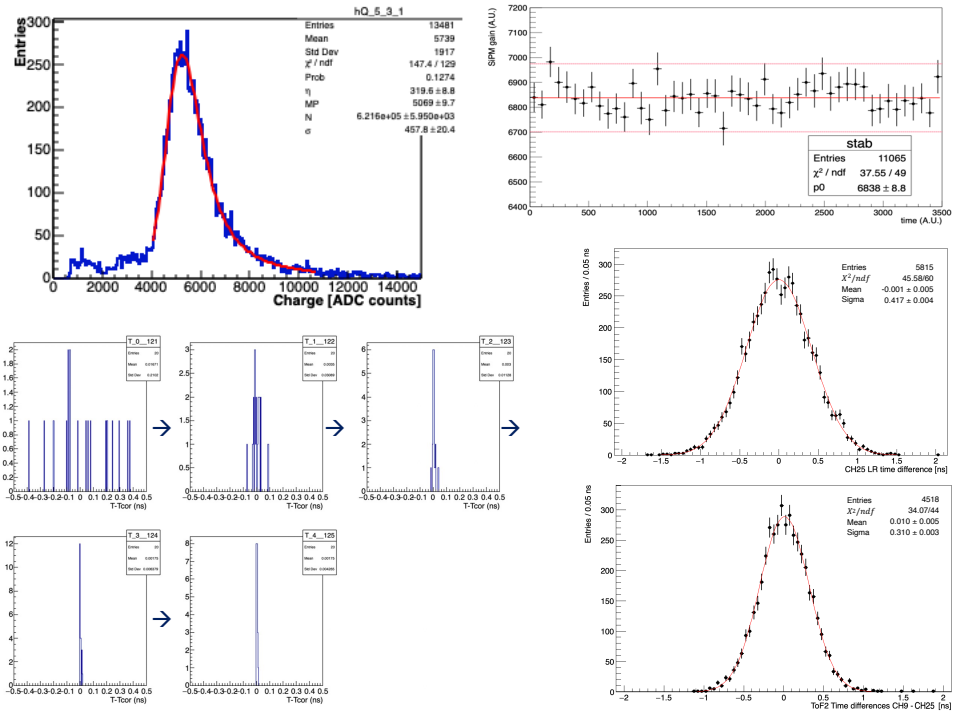

Figure 6: Top-left: example of MIP deposits in a crystal during VST with superimposed Landau–Gauss convolution fit. Top-right: relative SiPM gain stability over 2 weeks against MIP peak for the central channel (left), dashed lines represent ± 2% limits. Bottom-left: overview of the timing alignment procedure, histogram of offset residuals after 5 iterations of the alignment algorithm. Bottom-right: example distribution of MIP timing differences for the central crystal and example of timing differences between two channels after 2D ToF correction and timing alignment.

MIP tracks inside the calorimeter were reconstructed with a 2D fit in the plane orthogonal to the crystal axes (Fig. 5, right) and an iterative algorithm was used to adjust the relative timing offset between channels, accounting for the relative 2D Time of Flight (ToF) corrections, resulting in a relative alignment better than 5 ps RMS after 5 iterations (Fig. 6, bottom-left). A mean time resolution of order 210 ps was evaluated with MIPs for individual crystals, from the time difference between the left and right ROU readouts, as shown for the central crystal (Fig. 6, middle-right). Timing difference distributions between channels (Fig. 6, bottom-right), after ToF correction, are well centred around zero, providing consistent results with the simpler time differences between SiPMs.

The 2D tracks reconstructed by Module-0 are cross checked against the ones provided by the CRT, whose modules are placed above and below the calorimeter (Fig. 5). An algorithm to reconstruct this slope from the optical transport timing differences on the crystal matrix is currently being developed for increased performance in evaluating longitudinal response of crystals. Reconstructed track slopes and the relative effects on energy and timing resolution are validated against the track longitudinal information provided by the CRT system.

4. Conclusions

In this paper an abridged description of the design and construction status of the Mu2e calorimeter was reported. The final design has been confimed after an intense R&D and qualification campaign for all calorimeter components. The downstream calorimeter disk assembly is currenty in progress at Fermilab.

5. Acknowledgements

This work was supported by the US Department of Energy; Istituto Nazionale di Fisica Nucleare, Italy; the Science and Technology Facilities Council, UK; the Ministry of Education and Science, Russian Federation; the National Science Foundation, USA; the Thousand Talents Plan, China; the Helmholtz Association, Germany; and the EU Horizon 2020 Research and Innovation Program under the Marie Sklodowska-Curie Grant Agreement Nos. 101003460, 101006726, 734303, 822185, and 858199. This document was prepared by members of the Mu2e Collaboration using the resources of Fermilab, a U.S. Department of Energy, Office of Science, HEP User Facility. Fermilab is managed by Fermi Research Alliance, LLC (FRA), acting under Contract No. DE-AC02-07CH11359.

Bibliography

[1] L. e. a. Bartoszek, "Mu2e technical design report," *ArXiv:1501.05241*, 2015.

[2] S. M. e. a. Bilenky, "Mu2e technical design report," *Phys. Lett. B, vol.67*.

[3] "The straw tube tracker for the mu2e experiment," *Nucl. Phys. B. Proc. Suppl., vol. 273-275, pp. 2530-2532, 2016*.

[4] N. Atanov *et al.*, "The Mu2e Calorimeter Final Technical Design Report," *arXiv:1802.06341*, 2018.

[5] N. e. a. Atanov, "Design and test of the Mu2e un-doped CsI + SiPM crystal calorimeter," *Nucl. Instrum. Meth. A 936, pp. 94-97, 2019*.

[6] D. e. a. Paesani, "Mu2e Crystal Calorimeter Readout Electronics: Design and Characterisation," *Instruments 2022, 6(4), 68*.

[7] "The Mu2e e.m. Calorimeter: Crystals and SiPMs Production Status, journal=IEEE TRANSACTIONS ON NUCLEAR SCIENCE, VOL. 67, NO. 6, JUNE 2020,"

[8] "Design and Status of the Mu2e Crystal Calorimeter," *IEEE TRANSACTIONS ON NUCLEAR SCIENCE, VOL. 65, NO. 8, AUGUST 2018*.

[9] "Design, assembly and operation of a cosmic ray tagger based on scintillators and sipms," *10.1016/j.nima.2022.167538*.

[10] "An automated qc station for the calibration of the mu2e calorimeter readout units," *10.1016/j.nima.2022.167811*.